Supplementary Materials for

General Theory and Observation of Cherenkov Radiation Induced by Multimode Solitons

M. Amin Eftekhar,[1] Helena E. Lopez-Aviles,[1] Frank W. Wise,[2] Rodrigo Amezcua-Correa,[1] Demetrios N. Christodoulides,[1*]

*Corresponding author. Email: m.a.eftekhar@knights.ucf.edu

Supplementary Note 1. Phase matching condition. In a parabolic multimode fiber, the propagation constants of the $(m,n)th$ mode are:

$$\beta_{mn} = k_0 n(\omega)\left[1-\frac{2(m+n+1)\sqrt{2\Delta}}{k_0 a n(\omega)}\right]^{\frac{1}{2}}, \quad \text{(S1.1)}$$

where $k_0 = \omega_0$ is the free space wavenumber at angular frequency ω_0, and $n(\omega)$ represents the frequency dependent refractive index of silica. Here, Δ is the relative index difference and a is the fiber core radius.

Equation (S1.1) can be approximated to first order as

$$\beta_{mn} = k_0 n(\omega) - (m+n+1)\sqrt{\frac{2\Delta}{a^2}}. \quad \text{(S1.2)}$$

The dispersion relation for a multimode soliton is

$$\beta_{s_{pq}}\left(\omega_{s_{pq}}\right) = \frac{\omega_{s_{pq}}}{c} n\left(\omega_{s_{pq}}\right) - (p+q+1)\sqrt{\frac{2\Delta}{a^2}} + \frac{1}{V}\left(\omega-\omega_{s_{pq}}\right) + \frac{\left|\beta_{pq}^{(2)}\right|}{2\tau^2}. \quad \text{(S1.3)}$$

The dispersion relation for a dispersive wave is

$$\beta_{mn}\left(\omega_{r_{mn}}\right) = \frac{\omega_{r_{mn}}}{c} n\left(\omega_{r_{mn}}\right) - (m+n+1)\sqrt{\frac{2\Delta}{a^2}}. \quad \text{(S1.4)}$$

The phase-matching condition between a soliton mode (p,q) and a dispersive wave in another mode (m,n) is

$$\beta_{s_{pq}}\left(\omega_{r_{mn}}\right) = \beta_{mn}\left(\omega_{r_{mn}}\right). \quad \text{(S1.5)}$$

Solving for $\omega_{r_{mn}}$ after substitution of Eqs. (S1.3) and (S1.4) in Eq. (S1.5) we obtain:

$$\omega_{r_{mn}}\left(\frac{n\left(\omega_{r_{mn}}\right)}{c}-\frac{1}{V}\right) = [(m+n)-(p+q)]\sqrt{\frac{2\Delta}{a^2}} + \frac{\omega_{s_{pq}}}{c} n\left(\omega_{s_{pq}}\right) - \frac{1}{V}\omega_{s_{pq}} + \frac{\left|\beta_{pq}^{(2)}\right|}{2\tau^2}. \quad \text{(S1.6)}$$

Supplementary Note 2. Predicted dispersive wave line locations of the first emitted multimode-soliton. Right after the soliton fission event, the first emitted multimode-soliton has a velocity of

$2.049 \times 10^8\ m/s$, and is located approximately at $1.597\ \mu m$ ($187.7\ THz$). Since the fiber has been excited on-axis, only modes with $(m+n)$ even have a contribution to the spectrum. Based on our theoretical model, the phase-matching condition is met for the frequencies shown in the Supplementary Table 1.

Supplementary Table 1. Locations of DW comb lines right after soliton fission. The predicted locations of dispersive-wave comb lines for the numerical results of Fig. 2.

$\boldsymbol{m+n}$	$\mathbf{f_{DW}}$ **(THz)**
0	368.9
2	450.8
4	495.9
6	529.6
8	557.7
10	581.8

There is an excellent agreement between these predicted frequencies and the spectrum obtained from gUPPE simulations (Fig. 2 of main text).

Supplementary Note 3. Predicted dispersive wave lines for the first red-shifted multimode-soliton compared to gUPPE simulations.

The unidirectional pulse propagator (UPPE) allows one to model beam propagation in highly nonlinear waveguides and supercontinuum generation in highly multimode MMFs in a global manner, accounting for all possible nonlinear effects. In this respect, the evolution of the vectorial electric field is comprehensively described by

$$\partial_z \vec{E}(k_\perp, \omega, z) = i k_z \vec{E}(k_\perp, \omega, z) + \frac{i\omega^2}{2\varepsilon_0 c^2 k_z} \vec{P}(k_\perp, \omega, z) - \frac{\omega}{2\varepsilon_0 c^2 k_z} \vec{J}(k_\perp, \omega, z). \qquad \text{(S2.1)}$$

where $k_z(k_\perp, \omega) = \sqrt{\omega^2\, \varepsilon(\omega)/c^2 - k_x^2 - k_y^2}$ and $\varepsilon(\omega)$ is the frequency dependent permittivity of the medium with c representing the speed of light. The waveguide is represented as a static contribution to polarization $\vec{P}$, and is implemented as an additional module for the simulator. Equation (S2.1) implicitly considers diffraction/waveguiding processes as well as dispersion and mode walk-off effects. Moreover, all the nonlinear interactions are included in the polarization and current terms, represented by $\vec{P}(k_\perp, \omega, z)$ and $\vec{J}(k_\perp, \omega, z)$ in (S2.1), respectively. The UPPE core was primed to account for all nonlinear phenomena such as self-phase and cross-phase modulation, four-wave mixing, third harmonic generation, shock-effects, Raman, etc. The nonlinear Kerr coefficient is $n_2 = 2.9 \times 10^{-20} m^2 W^{-1}$ and its Raman fraction is taken here to be f = 0.18 in the standard two-parameter response model. The wavelength dependence of the refractive index is provided through an appropriate Sellmeier series.

From gUPPE simulations, the group velocity of the first emitted multimode-soliton 1.5 cm after the multimode-soliton fission event is estimated to be $2.0465 \times 10^8\ m/s$ ($n_g = 1.4649$), which is slower because of Raman red-shifting. This same soliton is located at 161.2 THz (1.8598 μm). Supplementary Figure 1 shows the theoretical predictions and numerical simulations associated with the new dispersive wave lines for this slower multimode-soliton.

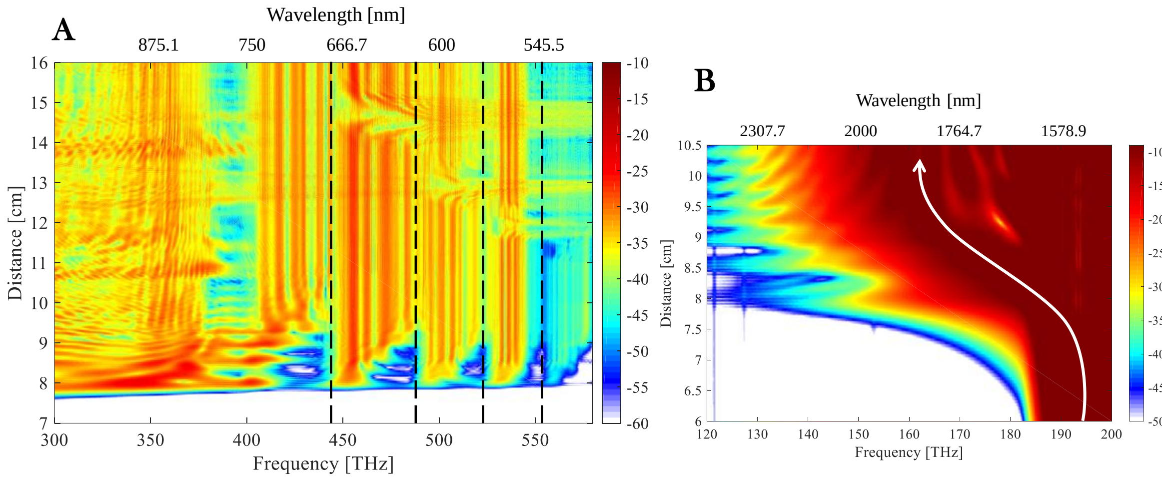

Supplementary Figure 1. **Theoretical prediction of DW lines of red-shifted soliton**. (**A**) The good agreement between the theoretically predicted dispersive wave lines associated with the red-shifted soliton (black dotted lines) and the numerical simulations. (**B**) A closer look at the spectral features of the first red-shifted multimode-soliton.

Predicted dispersive wave locations for the experimental results of a parabolic multimode fiber of the main text are described in Supplementary Table 2.

Supplementary Table 2. Locations of DW comb lines predicted for the experimental results. The predicted locations of dispersive-wave comb lines for the experimental results of Fig. 3.

$2K$	λ_{DW} (nm)
0	1689.0
2	675.3
4	608.2
6	566.3
8	536.5
10	513.0
12	494.3

where $2K = (m+n) - (p+q)$. These predicted wavelength lines are in excellent agreement with our experimental observations for $2K = 2,4,6,8,10,12$. The line for $2K = 0$ expected at 1689 nm, was not observed because of our maximum spectrometer range (1600 nm). Finally, the line observed at 735 nm corresponds to $(m+n) - (p+q) = 1$ and arises from an energy transition from the LP_{11} mode of the multimode soliton towards the LP_{01} mode associated with the dispersive wave at this wavelength. We believe that the LP_{11} mode in the multimode soliton was induced as a result of a slight misalignment of the input beam (from the central axis of the fiber) during excitation.

Supplementary Note 4. Spatiotemporal compression of the beam before the multimode-soliton fission event.

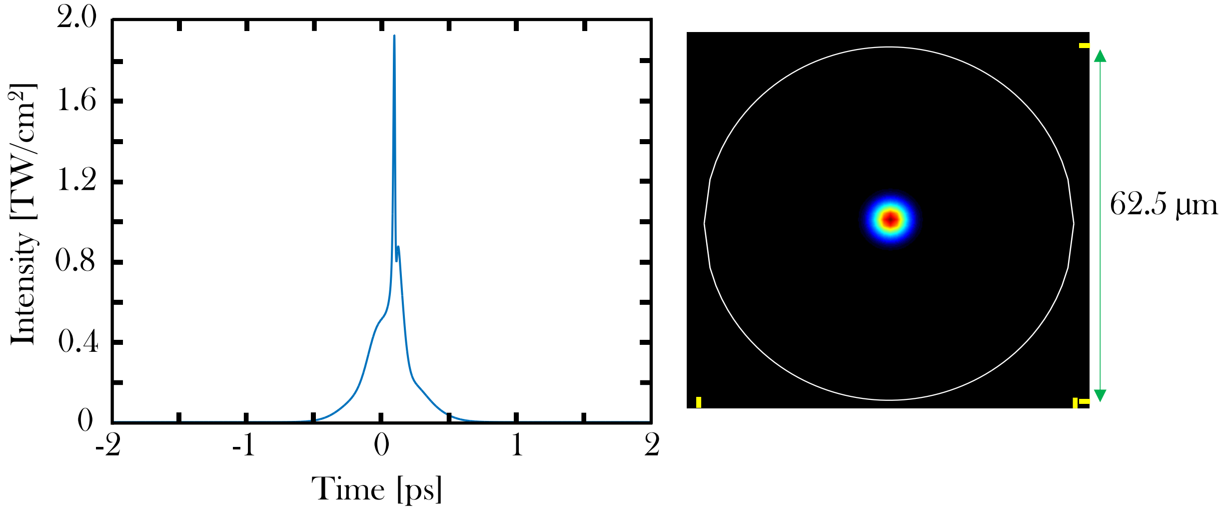

Supplementary Figure 2: **Spatiotemporal profile of the pulsed beam before soliton fission.** Significant compression of the pulsed beam in space and time right before the multimode-soliton fission event.

Supplementary Note 5. Phase-matching condition explaining the dispersive wave located at higher wavelengths. In both our theoretical model and numerical simulations, there is a dispersive wave line located in the long-wavelength region (~ 2.5 μm in Fig. 1 of main text). Supplementary Figure 3 implies that the phase-matching condition can be met at higher wavelengths, explaining this intriguing dispersive-wave observed in Fig. 1 of main text. Therefore, in multimode systems the dispersive wave frequency does not necessarily lie in the visible wavelengths, but can also be found in the long-wavelength edge.

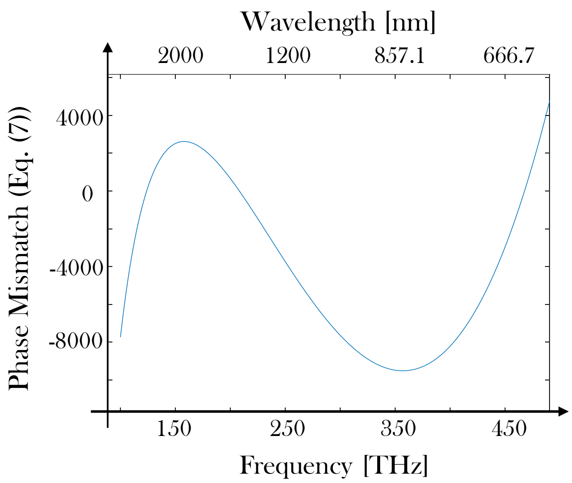

Supplementary Figure 3: **Phase-matching condition for DW line in NIR region.** Phase-matching condition explaining the dispersive wave line located in the 2-3 μm space of Fig. 1 in main text.

Supplementary Note 6. Multimode-soliton formation and fission in a step-index multimode fiber. Based on our theoretical model, for a step-index multimode fiber we expect a drift of the grouped sidebands away from each other and a formation of a continuum extending from 450 to 1000 nm is obtained (Supplementary Figure 4). This is because, unlike the parabolic multimode fiber, in this step-index multimode fiber we do not have an equidistant distribution of eigenvalues. Supplementary Figure 4 clearly shows that the dispersive wave grouping disappears in step-index multimode fibers.

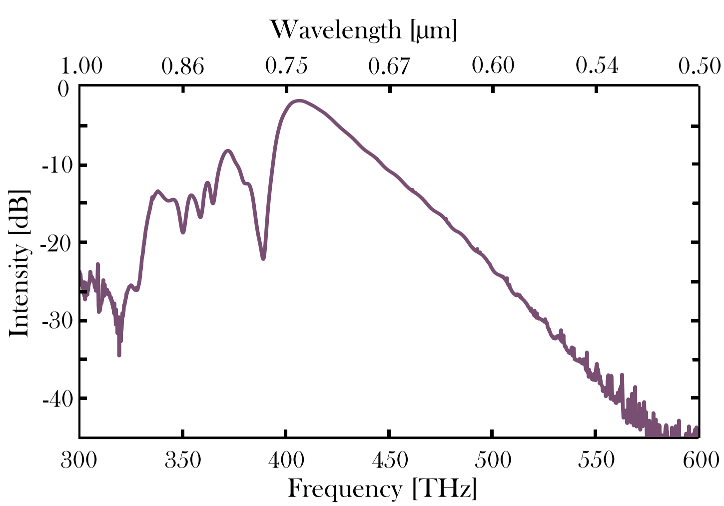

Supplementary Figure 4: **Broadband DW spectrum of a MM step-index fiber**. of Spectrum obtained from a gUPPE simulation showing the generation of a wideband dispersive wave as a result of the broadband phase-matching between many modes in a step-index multimode fiber. The fiber considered in our simulations has a core diameter of 105 μm and a numerical aperture NA=0.275.

The formation of multimode solitons in parabolic index MMFs can readily take place, given that the difference in group velocities is rather small. This explains why MM-soliton formation can observed at a relatively low power levels. Note, that for parabolic fibers, the multimode soliton fission event takes place approximately within the first 10-15 cm in the fiber. Similarly, our simulations carried out in step-index fibers also suggest a similar scenario: the MM-soliton fission occurs within approximately the first 10s of centimeter of propagation. The step-index fiber used in our experiments had a numerical aperture of 0.275, a diameter of 105 μm and hence at 1.55 μm, it supported ~1750 modes. Under these conditions, the maximum walk-off time delay between the lowest and the highest-order modes is ~ 25 ps for a length of 30 cm or so. In our experiments, we estimate that only first 10-20 modes are involved which approximately represent 1% of the total mode population. In this case, the maximum walk-off time between the first mode and 20^{th} mode is expected to be approximately 250-300 fs which is 2-3 times bigger than the pulse-width used in our experiments. Even though these values are higher than those expected from parabolic fibers, the multimode soliton locking still occurs because we used 700 kW that is more than enough to lock the modes by frequency shifting the participating modal components.